

BBA 73742

## Ion regulation of phosphatidylserine and phosphatidylethanolamine outside–inside translocation in human erythrocytes

Michel Bitbol, Pierre Fellmann, Alain Zachowski and Philippe F. Devaux

*Institut de Biologie Physico-Chimique, Paris (France)*

(Received 4 June 1987)

Key words Phospholipid, Flip-flop, Spin label, ESR, Calcium ion, intracellular, Vanadate, (Human erythrocyte)

In previous publications, we have shown, by using spin-labeled derivatives, that the translocation of phosphatidylserine and phosphatidylethanolamine from the outer to the inner monolayer of human erythrocyte membrane is a protein-mediated phenomenon, which requires hydrolysable  $\text{Mg}^{2+}$ -ATP. The inhibition by intracellular  $\text{Ca}^{2+}$  ( $0.2 \mu\text{M}$ ) or by extracellularly added vanadate ( $50 \mu\text{M}$ ) was reported (Seigneuret, M. and Devaux, P.F. (1984) *Proc. Natl. Acad. Sci. USA* 81, 3751–3755; Zachowski, A., Favre, E., Cribier, S., Hervé, P. and Devaux, P.F. (1986) *Biochemistry* 25, 2585–2590). The present article gives further insight into the effects of intracellular and extracellular ions on the aminophospholipid translocation in human erythrocytes. By measuring the cell ATP concentration, we now show that the inhibitory effect of intracellular calcium on spin-labeled aminophospholipid translocation is partly due to the ATP depletion, which follows the increased consumption by the calcium pump. However, a direct inhibitory effect of cytosolic  $\text{Ca}^{2+}$  on the aminophospholipid translocase can be demonstrated by measuring the initial rate of aminophospholipid translocation in the presence of variable amounts of intracellular calcium, at fixed ATP concentrations. Moreover, the transmembrane equilibrium distribution of phosphatidylserine and phosphatidylethanolamine are affected differently by  $\text{Ca}^{2+}$ : when cytosolic  $\text{Ca}^{2+}$  concentration is increased, alteration of phosphatidylethanolamine distribution begins as soon as the inward translocation is affected by  $\text{Ca}^{2+}$  (approx.  $50 \text{ nM}$ ), whereas phosphatidylserine distribution remains unchanged within a large inhibitory range of cytosolic  $\text{Ca}^{2+}$  concentrations and decreases above  $0.2 \mu\text{M}$  of free  $\text{Ca}^{2+}$  within the cytosol. Decrease of the intracellular  $\text{Mg}^{2+}$  concentration below its physiological value (approx.  $2 \text{ mM}$ ) results in the inhibition of aminophospholipid inward transport, whereas increase of  $\text{Mg}^{2+}$  concentration does not modify this transport. If  $\text{Mn}^{2+}$  is substituted for  $\text{Mg}^{2+}$ , part of the aminophospholipid translocation is maintained, whereas if  $\text{Co}^{2+}$  is substituted for  $\text{Mg}^{2+}$ , the rapid translocation is completely abolished. Concentrations as high as a millimolar of extracellular  $\text{Ca}^{2+}$ ,  $\text{Mg}^{2+}$  or  $\text{Mn}^{2+}$  have no effect on the aminophospholipid translocation. The less usual cations  $\text{Cr}^{3+}$ ,  $\text{Fe}^{2+}$ ,  $\text{Cu}^{2+}$ ,  $\text{Sn}^{2+}$  and  $\text{Eu}^{3+}$  are also ineffective. With extracellular  $\text{Ni}^{2+}$  or  $\text{Co}^{2+}$ , some inhibition can be observed, half inhibition by  $\text{Ni}^{2+}$  corresponding to  $500 \mu\text{M}$ . Vanadyl ( $\text{VO}^{2+}$ ), on the other hand, is a potent inhibitor of the aminophospholipid translocation when

Abbreviations PS, phosphatidylserine, PE, phosphatidylethanolamine, (0,2)PS, 1-palmitoyl-2-(4-doxylpentanoyl)phosphatidylserine, (0,2)PE, 1-palmitoyl-2-(4-doxylpentanoyl)phosphatidylethanolamine, (0,2) refers to the general nomenclature of spin labeled chains, 0 and 2 being, respectively, the number of methylene groups after and before the labeled position on the acyl chain Hepes, 4-(2-hydroxyethyl)-1-piperazineethane-

sulfonic acid EGTA, (ethylenedis(oxyethylenenitrilo))tetraacetic acid, EDTA, ethylene diaminetetraacetic acid, DMSO, dimethylsulfoxide, DIDS, 4,4'-diisothiocyanostilbene-2,2'-disulfonic acid

Correspondence P.F. Devaux, Institut de Biologie Physico-Chimique, 13 rue Pierre et Marie Curie, F-75005, Paris, France

applied on the extracellular surface, half-inhibition being reached around 30  $\mu\text{M}$ . Finally, the effect of vanadate ( $\text{VO}_4^{3-}$ ) was also investigated. Half-inhibition by extracellularly added vanadate was found at 50  $\mu\text{M}$ . However, pretreatment of the cells by a blocker of the anion carrier band 3 partly prevented the inhibitory property of vanadate. This suggests that vanadate effectively acts from the cell interior. Comparison between ionic regulation of the aminophospholipid translocation in human erythrocytes and the influence of ions on cell shape indicates that the asymmetry of phospholipid distribution is probably a major determinant in the control of the normal discoid shape.

## Introduction

The phospholipid distribution between the two leaflets of the erythrocyte membrane is asymmetric [1,2]. This is due, at least partly, to the selective translocation of phosphatidylserine and phosphatidylethanolamine, from the outer to the inner leaflet by an ATP-dependent carrier protein [3,4]. The active transport of aminophospholipids was discovered in 1984 using spin-labeled analogues of naturally occurring phospholipids [3]. Spin-labeled phospholipids with a short  $\beta$  chain ( $\text{C}_5$ ), bearing a doxyl group at the fourth position, incorporate rapidly and quantitatively into the erythrocyte outer leaflet; their reorientation within the membrane can be assessed by selective chemical reduction of the probes located on one membrane half. Using this technique, we showed large differences between the rates of transmembrane diffusion of aminophospholipids and of choline derivatives. A requisite for the rapid diffusion of aminophospholipids is the presence of ATP within the cells. The ATP requirement was confirmed by other laboratories using non-spin-labeled lipids [5,6]. The proteic nature of this selective inward translocation was demonstrated by its inhibition by protein reagents such as *N*-ethylmaleimide or vanadate, known inhibitors of ATPase. In order to produce and maintain phospholipid asymmetry, it is not necessary to postulate the existence of other enzymatic activities specific for phosphatidylcholine and sphingomyelin. A counter-diffusion process can explain the stable segregation between the aminophospholipids and the choline-containing phospholipids. The enzymatic activity, 'aminophospholipid translocase' [4], may be present not only in erythrocytes and their precursors, the reticulocytes [7], but also in a great variety of cells, such as platelets [5,8], lymphocytes [9] and fibroblasts [10].

The important role of two divalent cations was outlined in the previous studies. First, in resealed ghosts [3], the rapid aminophospholipid translocation requires the presence of  $\text{Mg}^{2+}$ , together with ATP. Secondly, this process is almost completely inhibited by micromolar amounts of free intracellular  $\text{Ca}^{2+}$  [4]. In the present article, the role of intracellular and extracellular cations on the rates of translocation and the equilibrium distribution of aminophospholipid analogues is further analyzed. We have also reinvestigated the inhibitory properties of vanadate anions and have shown that vanadyl cations which can be formed spontaneously from vanadate reduction are also potent inhibitors. However, inhibition by the two vanadium derivatives proceed by different pathways.

## Materials and Methods

**Buffers.** Two buffers were used: 140 mM NaCl/10 mM Hepes (pH 7.4) (buffer A) and 70 mM KCl/70 mM NaCl/1 mM EGTA/10 mM Hepes (pH 7.4) (buffer B). In some experiments, 1 or 2 mM EDTA was added to buffer A, or 20 mM inosine to buffer B (pH was adjusted to 7.4 whenever necessary). When the effect of  $\text{Mn}^{2+}$  or  $\text{Co}^{2+}$  was investigated, special attention was paid to the absence of residual amounts of other divalent cations. Buffer A was thus made with highly purified NaCl and its pH adjusted with highly purified NaOH (Normatom Prolabo, Paris, France).

**Erythrocytes.** Fresh human blood was obtained from healthy volunteers or from a local blood bank (Hôpital Cochin). Blood collected in EDTA was washed three times in 3 vol. of buffer A, by centrifugation at  $1000 \times g$ , and, for intracellular cation studies, once with 3 vol. of buffer B. The washed erythrocytes were stored on ice and used

within 6 h. All samples contained 5 mM of diisopropylfluorophosphate to minimize the hydrolysis of the spin-labeled phospholipids [9].

**Spin-labeling** Scheme I presents the spin-labeled phospholipids used. The polar head group, R, is serine or ethanolamine, and the molecules are termed (0,2)PS or (0,2)PE. These spin-labels were prepared enzymatically from the corresponding phosphatidylcholine spin-label [11], the latter being synthesized as described in Ref. 12. Membrane labeling was carried out as described in Ref. 3. The ESR spectra were recorded with a Varian E109 spectrometer. The transverse orientation of the spin-labeled phospholipids was assayed at 0°C, by ascorbate reduction of the labels exposed on the outer leaflet according to the method described in Ref. 3. Since several of the ions tested were paramagnetic, spectra were stored when necessary and a baseline subtraction carried out. At the maximum ion concentration used (approx. 1 mM), no spin-spin interaction took place between the paramagnetic cations  $Mn^{2+}$  or  $Ni^{2+}$  and the nitroxide probes. On the other hand, vanadyl added in the extracellular space was an efficient quencher of the spin-labels exposed on the outer face. As a result, the ESR signal observed in the latter case was directly associated with the amount of label on the inner layer.

**Control of divalent cation cytosolic content.** Erythrocytes were incubated, prior to spin-labeling, in buffer B at a 20% hematocrit in presence of 20  $\mu$ M calcium ionophore A23187 (from a 5 mM stock solution in DMSO/ethanol (2:1, v/v)). The high  $K^+$  concentration of buffer B (70 mM) was

used to prevent the net loss of cell potassium and cell shrinkage under the effect of added  $Ca^{2+}$ . Various amounts of  $CaCl_2$  were added in the incubation medium, so as to reach extracellular concentrations ranging between 0 and 1 mM. The cytosolic free calcium concentration may be computed by assuming: (i) that the affinity constant of the EGTA for  $Ca^{2+}$  in buffer B is  $1.32 \cdot 10^7 M^{-1}$  and (ii) that for the high ionophore concentration we used,  $[Ca^{2+}]_i$  and  $[Ca^{2+}]_o$  are the steady-state concentrations of ionized calcium in the cytosol and incubation medium, respectively,  $r \approx 1.5$  being the ratio of the intracellular and extracellular proton concentration [13]. Examples of respective values of  $[Ca^{2+}]_o$  and  $[Ca^{2+}]_i$ , computed according to the above assumptions are given in Table I.

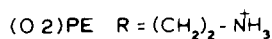
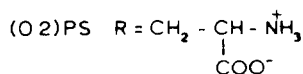
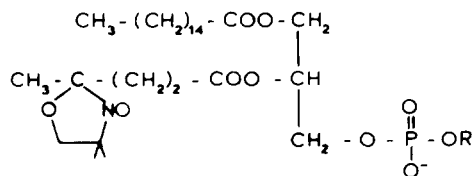
For magnesium monitoring, extracellular concentrations ranging between 0 and 4 mM were obtained by adding  $MgCl_2$  to similar cell suspensions as described above. Conversely, in order to achieve  $Mg^{2+}$  depletion, we used erythrocyte suspensions at 20% hematocrit in buffer A containing 2 mM EDTA and 20  $\mu$ M ionophore A23187.

When the effects of  $Mn^{2+}$  and  $Co^{2+}$  were investigated, two procedures were employed: (i) 0.1–1 mM of  $CoCl_2$  or  $Mn(acetate)_2$  was added to an erythrocyte suspension at 20% hematocrit in buffer A with 20  $\mu$ M ionophore A23187. (ii) The cells were first  $Mg^{2+}$ -depleted as described above, the suspension then washed twice in buffer A, and Mn and Co salts added under the same conditions as in (i).

Unless otherwise specified, all samples with ionophore and varying amounts of added salts were incubated 10 min at 37°C. The cells were then centrifuged at 4°C and either spin-labeled or used for intracellular ATP and magnesium concentration measurements.

**Measurements of intracellular magnesium concentration.** 20  $\mu$ l packed erythrocytes were first separated from their incubation medium by centrifugation in  $Mg^{2+}$ -free di-*n*-butylphthalate. The supernatant was carefully removed and the cells were hemolysed in 50 vol of 0.4%  $Mg^{2+}$ -free trichloroacetic acid. Magnesium concentration in the resulting solution was measured by atomic absorption spectrometry (Instrumentation Laboratory 457).

**Measurements of cellular ATP content** Cell ATP



Scheme I

TABLE I

COMPUTED VALUES OF  $[Ca^{2+}]_o$  (EXTRACELLULAR FREE CALCIUM CONCENTRATION) AND  $[Ca^{2+}]_i$  (INTRACELLULAR CALCIUM CONCENTRATION), FOR GIVEN CONCENTRATIONS OF ADDED CALCIUM CHLORIDE IN BUFFER B WITH IONOPHORE

	CaCl <sub>2</sub> (mM)							
	0.1	0.2	0.3	0.4	0.5	0.7	0.9	1
$[Ca^{2+}]_o$ ( $\mu$ M)	0.008	0.018	0.031	0.048	0.076	0.177	0.678	8.7
$[Ca^{2+}]_i$ ( $\mu$ M)	0.018	0.04	0.07	0.108	0.17	0.4	1.52	19.6

was extracted with 0.1% trichloroacetic acid and measured by the firefly luminescence test [14]. The test kit was purchased from LKB-Wallac (LKB-Wallac ATP assay kit). The photon emission was measured on a Lumacounter M2080.

**Control of extracellular ions.** 1 vol. of pelleted cells was added to 1 vol. of buffer A supplemented with the desired ion concentration from a 10-fold concentrated solution in buffer A. After 15 min incubation at room temperature with the ions, samples were cooled at 4°C, centrifuged and spin-labeled. For vanadate, the incubation medium contained 1 mM EDTA in order to chelate any vanadyl cation formed. For the investigation of vanadyl, in some experiments after incubation without EDTA and centrifugation, samples were resuspended in 10 vol. of buffer A, containing 1 mM EDTA, in order to chelate all vanadyl ions on the extracellular medium. After 15 min incubation the latter samples were centrifuged again and spin-labeled.

**Treatment with DIDS.** Washed erythrocytes were resuspended at a 25% hematocrit in buffer A containing 0.3 mM DIDS (Sigma). After 45 min at 37°C, cells were centrifuged before use. A control incubation without DIDS was run in parallel.

**Binding of radioactive vanadyl to erythrocytes.** 1 vol. of pelleted erythrocytes was added to 1 vol. of buffer containing various amounts of  $VO^{2+}$ . [ $^{48}V$ ]Vanadyl (Amersham) was used as a tracer. After 15 min incubation at room temperature, the cell suspension was centrifuged and an aliquot was sampled from the supernatant for scintillation counting. The pellet was resuspended in a 10-fold excess of buffer (without  $VO^{2+}$ ), centrifuged again and an aliquot of the supernatant counted. This procedure was repeated once.

**Membrane solubilization and chromatography.** 6

ml of washed, pelleted erythrocytes were added to 6 ml of 1 mM  $VOSO_4$  (containing  $^{48}VO^{2+}$ ) in buffer A and incubated for 15 min at room temperature. The suspension was centrifuged and the cells lysed in 10 vol. of 10 mM Tris (pH 7.4). The final pellet was brought to 1% (w/v) SDS and applied onto a 1 × 46 cm Sepharose 6B-prepacked column (Pharmacia), equilibrated in 1% SDS/10 mM Tris (pH 7.4). The elution rate was 4.5 ml per h and 0.6-ml fractions were collected at room temperature. Absorbance spectra (220–320 nm) were recorded with each fraction for protein assay. An aliquot of each fraction was sampled for scintillation counting.

## Results

### *Effects of intracellular divalent cations on the aminophospholipid translocation*

**Intracellular calcium.** The ESR signal of nonreducible (0,2)PS and (0,2)PE, corresponding to the fraction of label present at the inner face of the bilayer, was measured after different incubation periods. In Fig. 1(a), the nonreducible fraction of (0,2)PS is plotted as a function of incubation time for three concentrations of added calcium,  $t = 0$  being the instant when the spin-labels are mixed with the erythrocyte suspension. 1 mM of added calcium (i.e., 19.6  $\mu$ M of intracellular  $Ca^{2+}$ ) inhibits almost completely the active translocation process. As already reported [4], in the presence of ionophore A23187, the translocation of the aminophospholipid analogues is slowed down by the addition of calcium. Fig. 1(b) is the control experiment with  $Ca^{2+}$ , but without ionophore: extracellular calcium has no effect on (0,2)PS translocation.

Even though (0,2)PE is transported at a slower

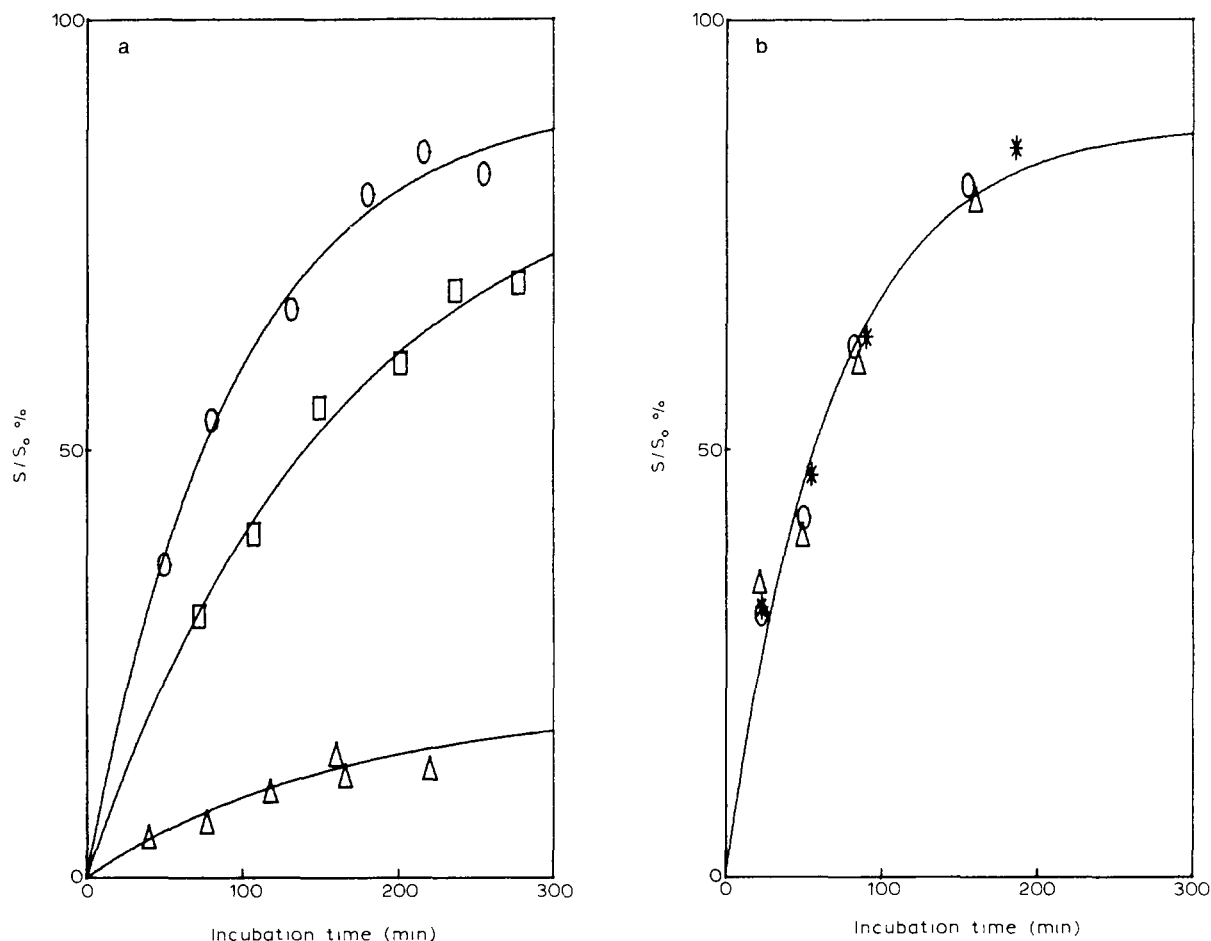


Fig 1 Non-reducible (0,2)PS fraction versus incubation time of the erythrocytes with the spin label. Incubations were carried out at  $0^{\circ}\text{C}$  (a) The incubation medium contains 1 mM EGTA and ionophore. The added calcium concentrations are 0 ( $\circ$ ), 0.5 ( $\square$ ) or 1 mM ( $\triangle$ ) (b) The incubation medium is the same as in (a), but it does not contain ionophore. The added calcium concentrations are 0 ( $\circ$ ), 1 ( $\triangle$ ) and 1.4 mM ( $*$ )

rate than (0,2) PS for each fixed amount of added calcium, the inhibitory effect of calcium is the same for (0,2)PE and (0,2)PS. This is shown in Fig. 2, wherein the initial rates of transport of each label for any concentration of added calcium are referred to the rate of the same label at 0 mM added calcium. The initial rates of translocation were deduced from the initial slopes of the curves which are instanced in Fig. 1.

*Effect of intracellular calcium on the equilibrium distribution of the spin-labeled aminophospholipids*  
The data plotted in Fig. 3 show that the effect of intracellular calcium on the equilibrium distribution is not the same for (0,2)PS and (0,2)PE. The fraction of (0,2)PS which is found at the inner face

of the membrane is not significantly modified by calcium loading up to approx. 0.5 mM added calcium (i.e.,  $0.17\ \mu\text{M}$  intracellular  $\text{Ca}^{2+}$ ). For higher calcium concentrations, the fraction of PS on the inner layer decreases regularly from approx. 80% to a value below 50%. Conversely, the fraction of (0,2)PE which is located at the inner layer decreases monotonically, without any threshold of added calcium. Note that this different response to calcium occurs, although no differences in calcium inhibition of the initial velocities was observed (see above).

*Intracellular  $\text{Ca}^{2+}$  and ATP concentration.* The cell ATP concentration was measured under the same experimental conditions as above. Data are

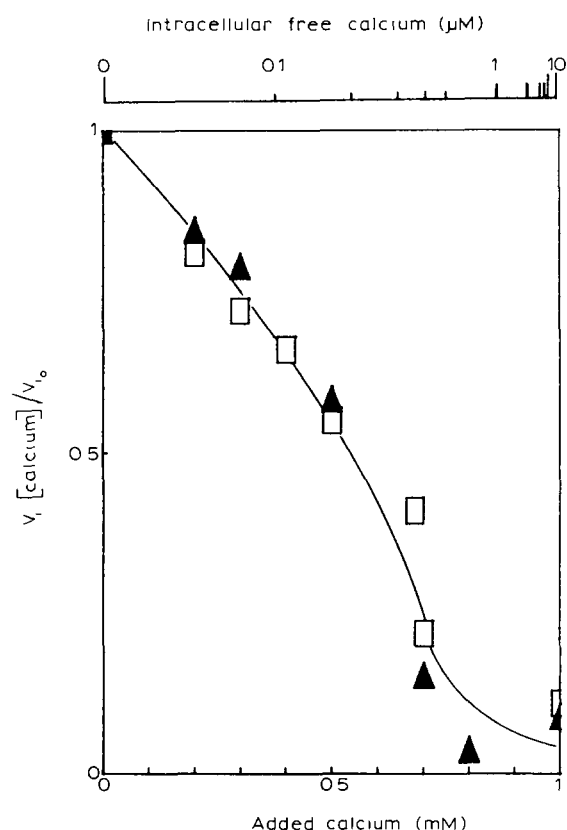


Fig 2 Initial rate of translocation of (0,2)PS ( $\square$ ) and (0,2)PE ( $\blacktriangle$ ) versus added calcium at fixed concentration of EGTA and ionophore. Data were referred to the initial rate observed in cells incubated with ionophore but without added calcium

shown in Fig. 4, where we have also plotted the ATP concentrations within erythrocytes incubated in buffer B with 20 mM inosine. The intracellular ATP concentration in the absence of inosine is dramatically decreased for added calcium concentrations above 0.5 mM, whereas it increases again above 0.8 mM of added calcium. In inosine-fed erythrocytes, the fall of ATP concentration takes place above 0.7 mM. Thus, the inhibitory effect of calcium on phospholipid translocation in erythrocytes without inosine (Figs. 1 and 2) might be due at least partly to a decrease of intracellular ATP.

*Intracellular calcium at fixed intracellular ATP concentration.*  $\text{Ca}^{2+}$  inhibits translocation and diminishes ATP levels; its effect on translocation is more than just the result of lowered ATP. We base this on the following (i) The intracellular

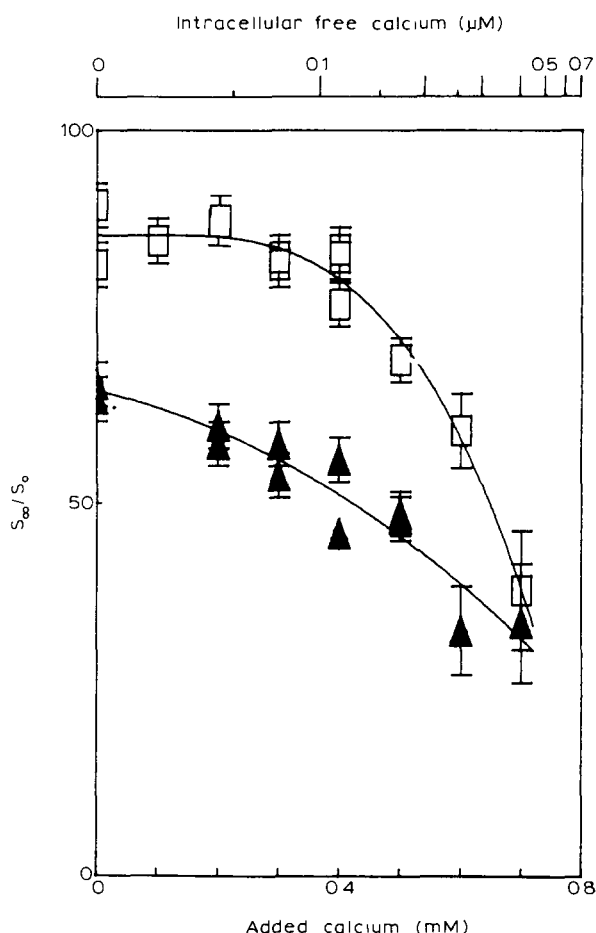


Fig 3 Non-reducible (0,2)PS ( $\square$ ) and (0,2)PE ( $\blacktriangle$ ) fractions at incubation time  $t_{\infty}$ , versus added calcium concentration.  $t_{\infty}$  is a time sufficient to reach approximately the asymptotes of the curves of Fig 1. Incubations were carried out at  $0^{\circ}\text{C}$  in a medium containing EGTA and ionophore. The curves are least-square fitted polynomials. Concentration of  $\text{Ca}^{2+}$  above 0.7 mM cannot be tested because  $t_{\infty}$  becomes of the order of magnitude of the hemolysis time in the incubation. The data in this figure were obtained from two separate experiments with blood from the same donor. Similar experiments were carried out with blood from other donors. The value of the asymptotic non-reducible spin-label fractions at zero calcium concentration varied between 80 and 90% for PS and between 60 and 80% of PE, according to the donor. However, for each blood sample, the curves indicated the same characteristic dependence with intracellular concentration, although the data cannot be reported on these curves because of the variation of the control levels

ATP concentration does not vary significantly for added calcium concentrations ranging between 0 and 0.4 mM (Fig. 4), whereas the initial velocity of

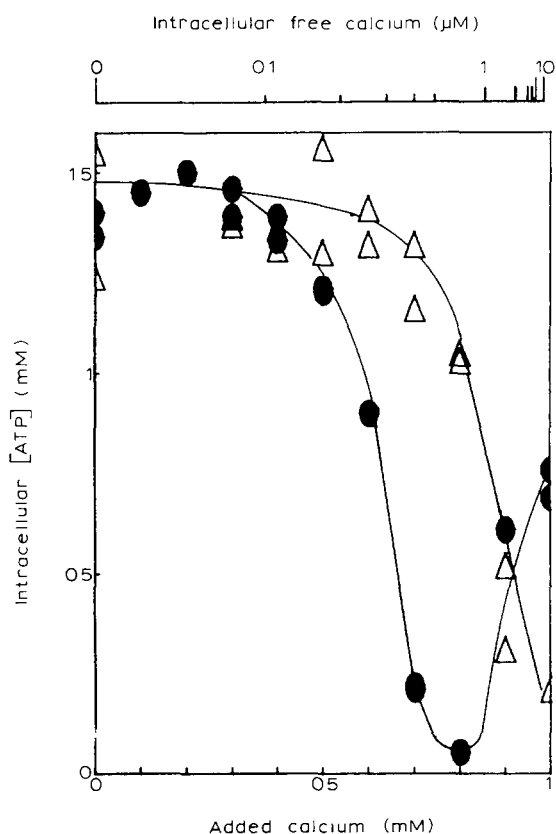


Fig 4 Intracellular ATP concentration (in mmol per liter of packed erythrocytes) versus calcium added. The values were obtained for red cells in a medium containing EGTA and ionophore, with ( $\Delta$ ) or without ( $\bullet$ ) 20 mM inosine

translocation decreases in the same range (Fig. 2). (ii) Inosine-loaded red cells (Fig. 4) maintain a constant intracellular ATP level up to 0.7 mM of added calcium. Yet, Table II shows that, even though the ATP level is maintained by inosine feeding, an inhibitory effect of calcium on phospholipid translocation persists. In a control experiment (not shown) we have verified that inosine alone has no effect on (0,2)PE translocation. (iii) Our conclusion concerning an intrinsic calcium inhibitory effect was reinforced by attempts to reverse it. Red cells were first incubated in the presence of ionophore and 0.7 mM calcium. Then calcium was removed from the cytosol by washing the cells in buffer B and incubating them for 10 min at 37°C with ionophore. The results concerning initial rates of (0,2)PE translocation are shown in Table III. They first show that calcium removal

TABLE II

INITIAL RATE OF (0,2)PS OUTSIDE-INSIDE TRANSLOCATION FOR RED CELLS IN BUFFER B WITH (+) OR WITHOUT (-) ADDITION OF 20 mM INOSINE IN THE PRESENCE OF IONOPHORE AND EITHER 0 OR 0.7 mM OF ADDED  $\text{CaCl}_2$

The results of ATP concentration are given  $\pm$  an estimated inaccuracy (about 10%).  $V_i$  is the initial rate of (0,2)PS translocation for the sample under consideration.  $V_i(0)$  is the initial rate of (0,2)PS translocation for the control sample. The inaccuracy is estimated from the standard deviations computed by mean-square fit of the kinetic curves instanced in Fig. 1

	$\text{CaCl}_2$ (mM)		
	0	0.7	
Inosine	+	-	+
ATP (mM)	$1.33 \pm 0.13$	$0.3 \pm 0.05$	$1.35 \pm 0.14$
$V_i/V_i(0)$	1	$0.4 \pm 0.1$	$0.77 \pm 0.1$

TABLE III

INITIAL RATE OF (0,2)PE TRANSLOCATION FOR RED CELLS INCUBATED IN BUFFER B IN THE PRESENCE OF IONOPHORE AND 0.7 mM OF ADDED CALCIUM, WITH (yes) OR WITHOUT (no) SUBSEQUENT REMOVAL OF THE ADDED CALCIUM

See Table II, for description of  $V_i/V_i(0)$ . The intracellular ATP concentrations were not measured on the same blood sample as the initial rate of (0,2)PE translocation, but identical experimental conditions were used.

	$\text{CaCl}_2$ (mM)		
	0	0.7	
Removal	yes	no	yes
$V_i/V_i(0)$	1	$0.16 \pm 0.1$	$0.59 \pm 0.1$
ATP (mM)	$1.4 \pm 0.14$	$0.26 \pm 0.05$	$0.33 \pm 0.05$

is not sufficient for ATP regeneration. Nevertheless, calcium removal allows one to recover a significant rate of (0,2)PE translocation. This demonstrates that for a low but constant cell ATP level (here about 0.3 mM), the presence of as little as  $0.4 \mu\text{M}$   $\text{Ca}^{2+}$  in the cytosol (corresponding to 0.7 mM added  $\text{CaCl}_2$ ) inhibits almost completely the outside-inside translocation of the aminophospholipid analogues.

In Fig. 5, the initial velocities of outside-inside (0,2)PS translocation are plotted versus (0,2)PS concentration for 0 and 1 mM of added calcium. Here, the ATP level of erythrocytes with 0 mM

calcium has been adjusted to the same level (i.e., 0.75 mM ATP) as that of erythrocytes with 1 mM calcium, by incubating the former in buffer A without ionophore, during 3 h at 37°C. The initial rates are much lower for red cells incubated with calcium than for controls. The maximum velocity ( $V_m$ ) and the apparent affinity ( $K_m$ ) of the translocation were computed by using the Woolf-Hofstee linearization, for both samples. This led to  $V_m = 4.5 \pm 0.2$  nmol of (0,2)PS/h per mg of membrane proteins and  $K_m = 16 \pm 1.4$   $\mu$ M for 0 mM added calcium, whereas  $V_m = 0.87 \pm 0.3$  nmol of (0,2)PS/h per mg of membrane proteins and  $K_m = 30 \pm 19$   $\mu$ M for 1 mM calcium. Notwithstanding considerable inaccuracies, intracellular calcium loading decreases  $V_m$ , while it does not change  $K_m$  significantly.

**Intracellular  $Mg^{2+}$ .** The initial rate of (0,2)PS translocation has been measured for several intracellular magnesium concentrations (Table IV).

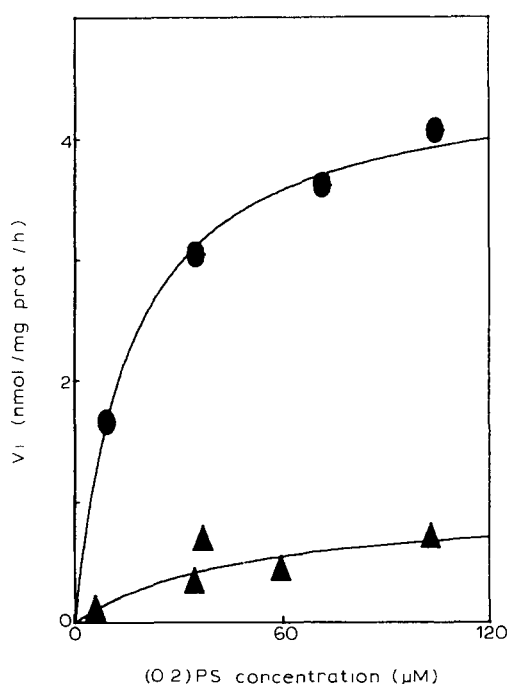


Fig 5 Initial rate of (0,2)PS translocation as a function of the amount incorporated in the erythrocyte membrane (expressed in  $\mu$ mol (0,2)PS per l of packed erythrocytes), for two concentrations of added calcium in the incubating medium containing EGTA and ionophore 0 (●) and 1 mM (▲). The curves were drawn using the Michaelis-Menten law, with parameters  $V_m$  and  $K_m$  as indicated in the text

Under our experimental conditions, no ATP depletion occurs, irrespective of the magnesium content of the cells. The initial rate of translocation is a steep but saturable, increasing function of the cell magnesium content. The saturation occurs in the vicinity of the physiological concentration of intracellular magnesium. Note that red cells are partially magnesium-depleted under the conditions used for calcium loading (i.e., 10 min of incubation at 37°C, with EGTA and ionophore). Other measurements (not shown) demonstrated that this partial magnesium depletion does not depend on the amount of added calcium in the incubation medium.

**Intracellular  $Mn^{2+}$  and  $Co^{2+}$**  The initial rate of (0,2)PS translocation has been measured when either  $Mn^{2+}$  or  $Co^{2+}$  are introduced in the intracellular medium (Table V). In the presence of 1 mM of either  $Mn^{2+}$  or  $Co^{2+}$ , without preliminary extraction of  $Mg^{2+}$ , the initial rate of aminophospholipid translocation is partially inhibited, to about one-third of the control. But when preliminary extraction of  $Mg^{2+}$  is performed, the behavior of  $Mn^{2+}$ -loaded erythrocytes departs from that of  $Co^{2+}$ -loaded ones.  $Mn^{2+}$  loading of the cells enables one to recover part of the transport activity which vanishes after  $Mg^{2+}$  depletion (initial velocity in  $Mg^{2+}$ -depleted –  $Mn^{2+}$ -loaded cells: about one-sixth of the control). On the contrary,  $Co^{2+}$  loading of the cells does not yield any recovery of the transport activity of  $Mg^{2+}$ -depleted cells. These differences are not accounted for by any significant difference in the cell ATP content.

#### *Effects of extracellular ions on the aminophospholipid translocation*

**Partial inhibition by multivalent cations.** Many cations, when present at 500  $\mu$ M in the extracellular medium, do not affect the reorientation of (0,2)PS in the red cell membrane. These are:  $Ca^{2+}$ ,  $Mg^{2+}$ ,  $Mn^{2+}$ ,  $Cr^{3+}$ ,  $Fe^{2+}$ ,  $Cu^{2+}$ ,  $Sn^{2+}$  and  $Eu^{3+}$ . On the other hand, we have found some effect of  $Co^{2+}$  and  $Ni^{2+}$ . With the latter ion, the half-inhibition was obtained with approx. 500  $\mu$ M (see Fig. 6); while 500  $\mu$ M  $Co^{2+}$  corresponded to 20% inhibition.

**Effect of vanadyl ( $VO^{2+}$ ).** Externally added vanadyl is an effective inhibitor of the



TABLE IV

## INITIAL RATES OF TRANSLOCATION OF (0,2)PS ACCORDING TO THE INTRACELLULAR MAGNESIUM CONTENT

Red cells were incubated 10 min at 37°C in buffer A with (+) or without (–) ionophore, with different chelators (EGTA or EDTA), and with or without added  $\text{MgCl}_2$ . The concentrations of ATP and magnesium are expressed in mmol per liter of packed erythrocyte. The corresponding measurements are not performed on the same samples, but under identical experimental conditions. For description of  $V_i/V_i(0)$  see Table II n.d., not determined. (The intracellular magnesium concentration was not measured after incubation with ionophore and EDTA 2 mM. However, it is known that under such conditions the red cells are severely  $\text{Mg}^{2+}$ -depleted)

Chelator	None	1 mM EGTA	2 mM EDTA	1 mM EGTA
Ionophore	–	+	+	+
$\text{MgCl}_2$ (mM)	0	0	0	0.4
$[\text{Mg}^{2+}]_i$ (mM)	$2.1 \pm 0.02$	$1.28 \pm 0.02$	nd	$2.61 \pm 0.02$
ATP (mM)	$1.16 \pm 0.12$	$1.39 \pm 0.14$	$1.27 \pm 0.13$	$1.28 \pm 0.13$
$V_i/V_i(0)$	1	$0.61 \pm 0.08$	$0.04 \pm 0.03$	$0.99 \pm 0.1$

aminophospholipid translocation. Fig. 7 shows the dose-response curve. Half-inhibition of the initial rate is obtained around 30  $\mu\text{M}$ . Yet the concentration range where the inhibition occurs is large, between 10 and 500  $\mu\text{M}$ . We suspect that several mechanisms are involved. In particular, vanadyl could be partially oxidized into vanadate ( $\text{VO}_4^{3-}$ ), which in turn could be transported in the cell interior by band 3 protein. Addition of DIDS, which is known to partially inhibit the ion uptake by band 3 protein [15], does not modify the dose-response curve obtained with vanadyl (not shown). On the other hand, when erythrocytes are washed in EDTA-containing medium after the preincubation with  $\text{VO}^{2+}$ , the inhibition curve is drastically modified (see the dotted curve in Fig. 7). A residual inhibition of the aminophospholipid translocation still exists, but 50% inhibition requires approx. 1 mM  $\text{VO}^{2+}$ . This represents a 40-fold in-

crease when compared to the concentration required for 50% inhibition in the absence of EDTA.

At 100  $\mu\text{M}$   $\text{VO}^{2+}$ , the inhibition of the aminophospholipid translocation rate was assayed with (0,2)PS and (0,2)PE as well. The percentage of activity remaining was identical for either substrate.

*Effect of vanadate ( $\text{VO}_4^{3-}$ ).* Addition of vanadate to the incubation medium of erythrocytes led to a strong inhibition of the aminophospholipid translocation. The dose-response curve is shown in Fig. 7. Half-inhibition occurs at approx. 50  $\mu\text{M}$ . In order to assess the action of vanadate from the cell interior, erythrocytes were pre-treated with DIDS. Addition of 200  $\mu\text{M}$  vanadate to the DIDS-treated cells indicated a residual translocation activity of 27% of the original activity, to be compared to a complete inhibition in the control

TABLE V

INITIAL RATES OF TRANSLOCATION OF (0,2)PS, WHEN  $\text{Mn}^{2+}$  OR  $\text{Co}^{2+}$  IS INTRODUCED IN THE RED CELL CYTOSOL

Red cells were incubated 10 min at 37°C in buffer A, in the presence of ionophore and of either 1 mM  $\text{Mn}(\text{acetate})_2$  or  $\text{CoCl}_2$ . Two situations were investigated: in one of them, preliminary extraction of intracellular  $\text{Mg}^{2+}$  with EDTA was performed, while in the other 1 mM,  $\text{Mn}^{2+}$  or  $\text{Co}^{2+}$  was added directly n.d., not determined

	No $\text{Mg}^{2+}$ extraction			$\text{Mg}^{2+}$ extraction		
$\text{CoCl}_2$	–	–	+	–	–	+
$\text{Mn}(\text{Ac})_2$	–	+	–	–	+	–
$V_i/V_i(0)$	1	$0.27 \pm 0.07$	$0.3 \pm 0.1$	$0.04 \pm 0.03$	$0.16 \pm 0.05$	$0.03 \pm 0.03$
ATP (mM)	$0.98 \pm 0.10$	$0.93 \pm 0.09$	$0.92 \pm 0.09$	nd	$0.92 \pm 0.09$	$0.76 \pm 0.08$

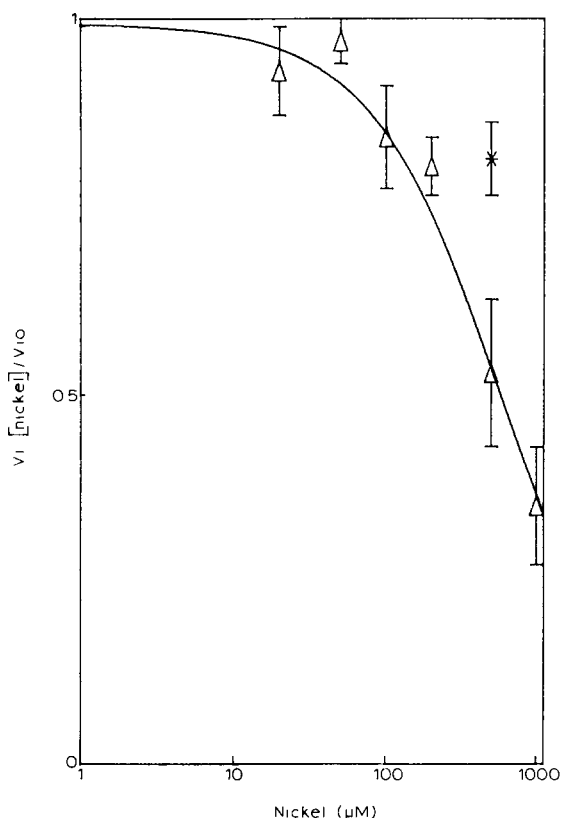


Fig 6 Initial rate of translocation of (0,2)PS versus extracellular nickel ion concentration (logarithmic scale). Data were referred to the initial rate in a control without added ions (\*). represents the inhibition obtained with 500  $\mu\text{M}$   $\text{CoCl}_2$  in the incubation medium

run without pretreatment with DIDS. This partial recovery of the activity is in accordance with a partial (approx. 60%) inhibition of vanadate uptake after treatment by DIDS [15]. Control of vanadate chemical stability within erythrocytes was carried out by ESR spectroscopy. For that purpose, pelleted cells were lysed by sonication and vanadate to vanadyl conversion was monitored by the intensity of the ESR spectrum associated with vanadyl ions bound to hemoglobin [15]. At 20°C, 20% of the vanadate was converted to vanadyl in 15 min; at 4°C, 8% of conversion only was measured in 1 h.

**Vanadyl binding to erythrocyte membranes.** We have carried out a few experiments with radioactive [ $^{48}\text{V}$ ]vanadyl to determine tentatively to which proteins the ions bind. After the binding step, the cells were lysed and the membrane were solubi-

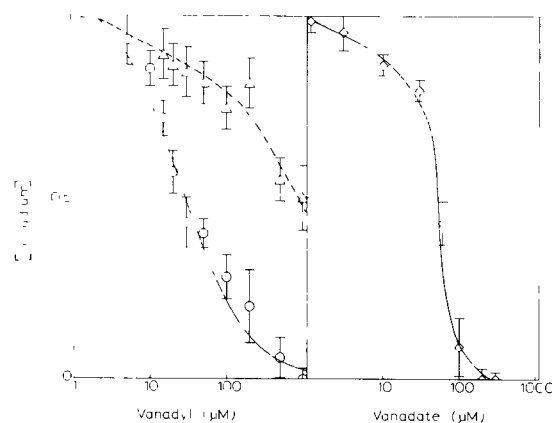


Fig 7 Inhibition of (0,2)PS translocation by vanadyl (left panel) or vanadate (right panel) ions. Concentrations (logarithmic scale) correspond to the amounts initially added in the incubation medium. For vanadyl ions, cells were washed in a buffer without (O) or with ( $\Delta$ ) EDTA before translocation assay

lized prior to gel chromatography on a Sepharose 6B-Cl column. The vast majority of the radioactivity was recovered at the elution volume, suggesting that the main binding of  $\text{VO}^{2+}$  takes place on the phospholipids. However, along with protein elution, radioactivity could be detected, peaking at components of relatively low molecular weight (under 50 000).

## Discussion

### *Biological relevance of the use of spin-labeled phospholipids*

It has been shown in previous publications [3,4] that the spin-labeled analogues used in the present investigation distribute themselves spontaneously across the erythrocyte bilayer according to their polar head group. The equilibrium distribution of those phospholipid analogues is identical to that of endogenous phospholipids [1,2]. The spontaneous redistribution of exogenous phospholipids in erythrocytes was confirmed recently by using long-chain radioactive phospholipids [6]. The translocation rates of paramagnetic aminophospholipids may be influenced by the presence of a short  $\beta$  chain bearing the nitroxide group. Yet it should be emphasized that the translocation rates of endogenous phospholipids cover a wide range,

for they depend on the length and saturation of the fatty acid chains involved [16]. Thus, we consider that the spin-labeled aminophospholipids used herein are reliable reporters of ion influence on the translocation rates of naturally occurring aminophospholipids.

#### *Role of intracellular $\text{Ca}^{2+}$*

Intracellular  $\text{Ca}^{2+}$  inhibits the translocation of both aminophospholipids (PS and PE). Half-inhibition is obtained at a concentration of 0.2  $\mu\text{M}$ ; however, the inhibitory effect of calcium begins taking place for intracellular  $\text{Ca}^{2+}$  concentrations as low as 40 nM. As a comparison, the sodium pump requires 20  $\mu\text{M}$   $\text{Ca}^{2+}$  for 50% activity decrease [17]. The physiological concentration of intracellular free calcium is approx. 20 nM in erythrocytes [18], but at least 60% of the total cell calcium is bound and may be liberated by phosphorylation of phosphatidylinositol [19]. Thus, the red cell has a pool of bound calcium which might be released through certain metabolic events, and might inhibit the aminophospholipid translocase accordingly. This is likely to occur during cell ageing: the old cells are known to contain more calcium than the young ones [20].

The decrease in the outside-inside aminophospholipid translocation rate under intracellular  $\text{Ca}^{2+}$  loading is associated with a modification of the equilibrium distribution of the phospholipid analogues across the membrane (Fig. 3). Williamson et al. [21] reported a loss of the transmembrane phospholipid asymmetry in ghosts in the presence of 5–10  $\mu\text{M}$   $\text{Ca}^{2+}$ .

We have observed that the inhibition of aminophospholipid translocation rate yields a detectable change of (0,2)PS distribution only if this rate decreases by more than 50% of its control value, whereas (0,2)PE transbilayer distribution is modified as soon as the translocation rate is slightly inhibited. This difference in behavior between the two aminophospholipids may be accounted for if we assume that the steady-state transmembrane distribution of the phospholipids results from an equality between the number of molecules transported inwards and the number of molecules transported outwards. A simple model of such process has been presented in Ref. 22. In this model the inward and outward translocation

rates are  $k_i$  and  $k_o$ , respectively, and the transbilayer equilibrium distribution for a given phospholipid species is  $q_p$ . Although the model does not take into account the saturability of the inward transport [4], it leads to reasonable orders of magnitude for the relations between  $k_i$ ,  $k_o$  and  $q_p$ . Most importantly, it explains the mechanisms underlying the difference in behavior of the two aminophospholipids. Indeed, according to the model, when  $k_i/k_o \approx 1$ ,  $q_p$  is very sensitive to any variation of either  $k_i$  or  $k_o$ ; on the other hand, when  $k_i/k_o \gg 1$ ,  $q_p$  is almost invariable in a wide range of variation of this ratio. These predictions are consistent with our measurements. Under our experimental conditions, the ratio  $k_i/k_o$  is much greater than 1 for (0,2)PS whereas it is close to 1 for (0,2)PE.

The differences between PS and PE distribution changes induced by intracellular calcium loading suggest that the primary 'flywheel' of phospholipid asymmetry regulation is PE. It is only when cell metabolism is radically altered, leading among other consequences to considerable increase of the cytosolic calcium level, that PS physiological distribution might be disturbed.

Fig. 3 reveals that the intracellular fraction of aminophospholipid analogues decreases below 50% when more than 0.4  $\mu\text{M}$  of free calcium is present in the cytosol. If the phospholipid distribution is random in the absence of active translocation, one must conclude that the outer leaflet corresponds to a larger area. This is indeed the case with high intracellular calcium, since most cells are then in the echinocytic shape and the echinocytes are associated with a larger external area [23].

To study the mechanism by which intracellular calcium inhibits the aminophospholipid translocation, it was necessary to show that the inhibitory effect of calcium loading is not the mere consequence of ATP depletion. The red cell calcium pump is stimulated by intracellular  $\text{Ca}^{2+}$ . Some experimental conditions lead to ATP consumption by the calcium pump, thereby decreasing the intracellular ATP concentration [17,24]. Fig. 4 shows that this is the case in some of our experimental conditions, since we observe a deep minimum of cell ATP concentration for approx. 0.8 mM of added calcium. The biphasic phase of the ATP curve for erythrocytes incubated with

ionophore and various quantities of added calcium was reported and discussed in Ref. 24. The primary interest of this curve, in this report, is to indicate that aminophospholipid translocase inhibition by calcium is partly due to ATP depletion.

We have given evidence of the existence of a direct inhibitory effect of calcium. In particular, the aminophospholipid translocation rates with and without added calcium were compared under conditions such that cell ATP concentrations were brought to equality. This intrinsic calcium effect is probably due to an inhibition of the ATPase activity of the putative aminophospholipid translocase, rather than to a modification of the affinity of the aminophospholipids for their outer binding site on this protein: indeed calcium acts only when its concentration is increased in the intracellular medium. Moreover, the apparent  $K_m$  of the phospholipids for the carrier is not significantly changed by calcium loading, whereas the maximum velocity  $V_m$ , which depends both on the number of carrier protein copies and on their turnover rate, is decreased. The inhibition of the ATPase activity of the carrier by calcium, and of its turnover accordingly, might be due to substitution of Ca-ATP for Mg-ATP, which is the physiological substrate of the aminophospholipid translocase [3]. This is unlikely since it would imply that the affinity of Ca-ATP for the aminophospholipid  $Mg^{2+}$ -ATPase is several orders of magnitude greater than that of Mg-ATP; in the experiments the concentration of Ca-ATP formed is not sufficient to change significantly the Mg-ATP levels. Alternatively, the inhibition might be due to a  $Ca^{2+}$  activation of intracellular proteases, leading to the destruction of the aminophospholipid carrier. However, this is also unlikely since the inactivation by  $Ca^{2+}$  is reversible. This was demonstrated by our experiments showing that when calcium is extracted from the loaded cells, they recover a normal aminophospholipid transport activity, account being taken of the decrease of the ATP concentration they experienced during preliminary incubation with ionophore and calcium. Finally, the intrinsic inhibitory effect of calcium on the aminophospholipid outside-inside translocation might be related to the fact that  $Ca^{2+}$  affects lateral phase separation in phosphatidylserine-containing membranes [25]. Alter-

ations of PS surface concentration in the vicinity of the extracellular moiety of the aminophospholipid translocase could modify its functioning. But again this hypothesis is ruled out by the data in Fig. 1(b), showing that no inhibition of (0,2)PS translocation is observed when calcium is added without ionophore.

In conclusion, the inhibitory effect of  $Ca^{2+}$  on the aminophospholipid translocation is probably a direct effect on the ATPase site of the carrier.

#### *Role of intracellular $Mg^{2+}$ , $Mn^{2+}$ and $Co^{2+}$*

$Mg^{2+}$  was found to be essential for the aminophospholipid translocation to take place. The functioning of the aminophospholipid carrier thus bears close analogy with other membrane carriers, such as the calcium pump, which requires  $Mg^{2+}$  at some stage of its reaction cycle [26]. Decrease of cell magnesium content below the control value decreased the aminophospholipid translocation rate, whereas increasing this content at constant ATP level did not enhance the translocation rate. This result may have a physiological meaning: it was demonstrated that red cell magnesium content decreases with erythrocyte age [27]. This fact, together with cell calcium increase, might provoke disruption of phospholipid asymmetry in aged red blood cells, which in turn is able to induce recognition and phagocytosis by macrophages [28].

$Mn^{2+}$  and  $Co^{2+}$  are both inhibitors of the aminophospholipid translocation when they are introduced in the intracellular medium. However, the inhibitory power of these divalent cations is much weaker than that of  $Ca^{2+}$ . A difference between the effects of  $Mn^{2+}$  and  $Co^{2+}$  was found when preliminary extraction of  $Mg^{2+}$  was carried out.  $Mn^{2+}$  yields partial recovery of the transport activity which was lost as a consequence of  $Mg^{2+}$  extraction, whereas  $Co^{2+}$  has no such property. These observations are consistent with the following interpretation: (i)  $Mn^{2+}$  and  $Co^{2+}$  inhibit the aminophospholipid transport at millimolar levels because they substitute to  $Mg^{2+}$  on ATP (which is itself millimolar in normal cells), and thus give rise to non-negligible amounts of Mn-ATP or Co-ATP. (ii) Mn-ATP is a substrate of the aminophospholipid carrier ATPase (still much less efficient than Mg-ATP) whereas Co-ATP is not a substrate at

all. The differences between  $\text{Co}^{2+}$  and  $\text{Mn}^{2+}$  will be further discussed below (see the discussion on the factors influencing cell morphology).

#### *Effects of vanadium derivatives*

Most ions added on the extracellular face of erythrocyte membranes which contain no ionophores have little effects on the aminophospholipids translocation.  $\text{Ni}^{2+}$  and  $\text{Co}^{2+}$  have a small inhibitory effect but only at a high concentration (approx. 1 mM). On the other hand, vanadium derivatives are rather potent inhibitors, since inhibition takes place around 20  $\mu\text{M}$  concentration. Under physiological conditions vanadium is found under two oxidation states: V(V) (vanadate,  $\text{VO}_4^{3-}$ ) and V(IV) (vanadyl,  $\text{VO}^{2+}$ ). When red cells are incubated with vanadate, aminophospholipid translocation is inhibited in a dose-dependent manner, especially in the concentration range 20–100  $\mu\text{M}$ . This inhibition is partly prevented by pre-treatment of the erythrocytes by DIDS, which suggests that vanadate acts from the cell interior, possibly by the substitution of phosphate by vanadate. This was demonstrated for  $(\text{Na}^+ + \text{K}^+)\text{-ATPase}$  [29] and other phosphatases [30]. Indeed, pentavalent vanadium can adopt a trigonal bipyramidal structure resembling the transition state of the phosphate group during ATP hydrolysis [31]. Thus, inhibition by vanadate suggests that a phosphorylated intermediate exists during the turnover of the protein.

The effect of vanadyl ions on the aminophospholipid translocase was also investigated. When compared to the dose response curve obtained with vanadate, the curve resulting from  $\text{VO}^{2+}$  addition is significantly different: inhibition by vanadyl is more pronounced at low dose but less important at high doses. Thus, it seems unlikely that the two states of vanadium use the same pathway to inhibit the aminophospholipid translocation. However, it is most probable that  $\text{VO}^{2+}$  added to the cells as soluble ions is transformed during incubation into insoluble hydrolysed complexes [32].

In the literature, few reports deal with enzyme inhibition by vanadyl ions. Yet several enzymes whose substrate is phosphorylated appear to be sensitive to the presence of this cation; examples are alkaline phosphatase, adenylate cyclase and

ribonuclease while other enzymes such as  $(\text{Na}^+ + \text{K}^+)\text{-ATPase}$  are quite insensitive to V(IV) [30]. It must be emphasized that vanadyl inhibits translocation of PS and PE to the same extent, although these two substrates exhibit different apparent  $K_m$  values for the aminophospholipid translocase [4]. Thus, vanadyl behaves as a non-competitive inhibitor of the translocation system with an apparent inhibition constant of approx. 25  $\mu\text{M}$  (50% inhibition). Possibly, vanadyl acts through an interaction on the lipid phase [33]; in fact, we have shown that [ $^{48}\text{V}$ ]vanadyl binds mostly to the lipids.

#### *Cell morphology, ions and aminophospholipid translocation*

Several authors have studied the influence of intra- or extracellular ions on erythrocyte morphology. It is tempting to try to correlate ion influence on cell morphology and ion influence on the aminophospholipid translocation.

The alteration of the normal biconcave disk-shape of human erythrocytes or ghosts by intracellular  $\text{Ca}^{2+}$  is a well-documented fact [34]. The reason for such calcium-induced shape change has been extensively discussed: it is still unknown whether the crenating effect of calcium on red cell shape is related to its action on lipids or cytoskeletal proteins. Many authors have tended to promote as an explanation of this phenomenon the transmembrane potential [35], or the Gardos effect [20]. But it has been demonstrated that the calcium-induced shape change can equally be obtained without modifying either the transmembrane potential or the intracellular  $\text{K}^+$  content [36]. Looking at the literature, the effects of intracellular calcium on red cell shape may be divided into two groups: (i) leaky ghosts incubated with any cations crenate.  $\text{Ca}^{2+}$  is only more efficient than monovalent cations [36]. (ii) Ghost crenation induced by salts can be reverted if Mg-ATP is present at the inner face of the membrane, but addition of 1 mM  $\text{Ca}^{2+}$ , leading to Ca-ATP, prevents shape reversion by Mg-ATP, which is independent of spectrin phosphorylation [37].

An attempt to give a coherent explanation of the effects of calcium on ghost shape as described in Ref. 37, becomes possible at this point: (i) The lysis of erythrocytes, which is the first stage in the preparation of ATP-depleted white ghosts, results

in a partial loss of phospholipid asymmetry [38]. (ii) As long as the ionic strength of the incubating medium of the ghosts is low (lysis buffer), the state of the spectrin layer does not allow the bilayer to bend; but when the ionic strength is restored to higher levels a crenated shape is generated [39]. (iii) The addition of Mg-ATP to the incubation medium allows aminophospholipid translocation to take place, and recovery of both physiological phospholipid asymmetry and discocyte shape are obtained.

An important argument strengthening the previous interpretation is afforded by our data concerning the effect of divalent cations other than  $Mg^{2+}$ . When calcium is added, or when Co-ATP is substituted for Mg-ATP, the aminophospholipid translocase is inhibited and no recovery of asymmetry occurs. Thus, it can be understood that, under these conditions, crenated ghosts cannot revert towards the discocyte pattern [37]. On the other hand, substitution of Mn-ATP for Mg-ATP allows recovery of discocyte shape [37]. This closely parallels our findings concerning the possibility to substitute  $Mn^{2+}$  for  $Mg^{2+}$  as a substrate for the ATPase of the aminophospholipid carrier. One must notice at this point that the previous divalent cation substitution pattern, which is identical for both the shape recovery process and the aminophospholipid translocation, is quite unusual. In particular, it is completely different from the divalent cation substitution pattern of spectrin or lipid phosphorylation: in the latter processes, Co-ATP and not Mn-ATP can be substituted for Mg-ATP [37].

Finally, the inhibition of aminophospholipid translocation by vanadate parallels the inhibition of the ATP-dependent shape change of human erythrocytes as reported by Patel and Fairbanks [37]. Schrier et al. [40] have also reported an inhibition by vanadate of the red cell endocytosis produced by high concentrations of Mg-ATP. It is tempting to suggest that the latter phenomenon (red cell endocytosis) occurs after stomatocyte formation when an excess of lipids (PS and PE) continues to reach the inner layer, this is what one expects when the ATP concentration is increased above the physiological value.

## Acknowledgements

The authors thank Dr. G. Dagher (INSERM U7) for fruitful discussions concerning the physiology of divalent cations, and for having allowed us to use an atomic absorption spectrometer. We thank Mrs. P. Hervé for the gift of the spin labels and Dr. J. Kornblatt for carefully reading the manuscript. This work was supported by grants from the Ministère de la Recherche et de l'Enseignement Supérieur, the Centre National de la Recherche Scientifique (UA 526), the Institut National de la Santé et de la Recherche Médicale, the Université Paris VII and the Fondation pour la Recherche Médicale.

## References

- 1 Bretscher, M S (1972) *J Mol Biol* 71, 523–528
- 2 Verkleij, A.J., Zwaal, R F A., Roelofsen, B., Comfurius, P., Kastelijn, D. and Van Deenen, L L M (1973) *Biochim. Biophys Acta* 323, 178–193
- 3 Seigneuret, M and Devaux, P F (1984) *Proc Natl Acad Sci USA* 81, 3751–3755
- 4 Zachowski, A., Favre, E., Cribier, S., Hervé, P. and Devaux, P F (1986) *Biochemistry* 25, 2585–2590 and 7788
- 5 Daleke, D.L. and Huestis, W H (1985) *Biochemistry* 24, 5406–5416
- 6 Tilley, L., Cribier, S., Roelofsen, B., Op den Kamp, J A F and Van Deenen, L L M (1986) *FEBS Lett.* 193, 21–27
- 7 Zachowski, A., Craescu, C T., Galacteros, F and Devaux, P F (1985) *J Clin Invest* 75, 1151–1156
- 8 Sune, A., Bette-Bobillo, P., Bienvenue, A., Fellmann, P and Devaux, P.F. (1987) *Biochemistry* 26, 2972–2978
- 9 Zachowski, A., Hermann, A., Paraf, A and Devaux, P F (1987) *Biochim Biophys Acta* 897, 197–200
- 10 Martin, O C and Pagano, R E (1987) *J Biol Chem*, in the press
- 11 Comfurius, P. and Zwaal, R F A (1977) *Biochim Biophys Acta* 488, 36–42
- 12 Keana, J F.W. and La Fleur, L E (1979) *Chem Phys Lipids* 23, 253–266
- 13 Ferreira, H G and Lew, V L (1976) *Nature* 269, 47–49
- 14 Brown, A M (1982) in *Red Cell Membranes — A Methodological Approach* (Ellory, J C and Young, J D., eds), pp 223–238, Academic Press, London
- 15 Cantley, J C, Jr and Alsen, P (1979) *J. Biol Chem* 254, 1781–1784
- 16 Middelkoop, E., Lubin, B H., Op den Kamp, J A F and Roelofsen, B (1985) *Biochim Biophys Acta* 855, 421–424
- 17 Brown, A M and Lew, V L (1983) *J Physiol* 343, 455–493
- 18 Lew, V L., Tsien, R Y., Miner, C and Bookchin, R M (1982) *Nature* 298, 478–481
- 19 Chauhan, V P S and Brockerhoff, H (1986) *Biochem Biophys Res Commun.* 136, 288–293

- 20 Shiga, T, Sekiya, M., Maeda, N, Kon, K and Okazari, M (1985) *Biochim Biophys Acta* 814, 289–299
- 21 Williamson, P., Algarin, L., Bateman, J, Choe, H R. and Schlegel, R A (1985) *J Cell Physiol* 123, 209–214
- 22 Hermann, A and Müller, P (1986) *Biosci Rep* 6, 185–191
- 23 Sheetz, M P and Singer, S J (1974) *Proc Natl Acad Sci USA* 71, 4457–4461
- 24 Taylor, D, Baker, R and Hochstein, P (1977) *Biochem Biophys Res Commun* 76, 205–211
- 25 Ohnishi, S and Tokutomi, S (1981) in *Biological Magnetic Resonance* (Berliner, L W and Reuben, J, eds ), Vol 3, pp 121–153
- 26 Garrahan, P J and Rega, A F (1978) *Biochim Biophys Acta* 513, 59–65
- 27 Watson, W S, Lyon, T D B and Hilditch, T E (1980) *Metabolism* 29, 397–399
- 28 McEvoy, L, Williamson, P and Schlegel, R A (1986) *Proc Natl Acad Sci USA* 83, 3311–3315
- 29 Cantley, J C, Jr, Cantley, L G and Josephson, L (1978) *J Biol Chem* 253, 7361–7368
- 30 Macara, I G (1980) *Trends Biochem Sci* 5, 92–94
- 31 Lindquist, R N, Lynn, J L, Jr. and Lienhard, G E (1973) *J Am Chem Soc* 95, 8762–8768
- 32 Chasteen, N.D. (1981) in *Biological Magnetic Resonance* (Berliner, L.W and Reuben, J, eds ), Vol 3, pp 53–119
- 33 Amler, E, Teisinger, J, Svobodova, J and Vyskocil, F (1986) *Biochim Biophys Acta* 863, 18–22
- 34 Weed, R.I. and Chailley, B (1973) in *Red Cell Shape Physiology, Pathology, Ultrastructure* (Bessis, M, Weed, R I and Leblond, P F, eds ), pp 55–67, Springer-Verlag, New York
- 35 Herrmann, A., Muller, P. and Glaser, R (1985) *Biosci Rep* 5, 417–423
- 36 Bifano, A M, Novak, T S and Freedman, J C (1984) *J Membrane Biol* 82, 1–13
- 37 Patel, V.P and Fairbanks, G (1986) *J Biol Chem* 261, 3170–3177
- 38 Lange, Y, Gough, A and Steck, T L (1982) *J Membrane Biol* 69, 113–123
- 39 Stokke, B T, Mikkelsen, A and Elgsaeter, A (1986) *Eur Biophys J* 13, 203–218
- 40 Schrier, S L, Junga, I and Ma, L (1986) *Blood* 68, 108–1014